http://dx.doi.org/10.5012/bkcs.2013.34.5.1361

# Matrix Infrared Spectra and DFT Computations of $CH_2CNH$ and $CH_2NCH$ Produced from $CH_3CN$ by Laser-Ablation Plume Radiation

**Han-Gook Cho**

*Department of Chemistry, University of Incheon, Incheon 406-772, Korea. E-mail: hgc@incheon.ac.kr*
*Received November 22, 2012, Accepted February 5, 2013*

The smallest ketenimine and hydrogen cyanide *N*-methylide ($CH_2CNH$ and $CH_2NCH$) are provided from the argon/acetonitrile matrix samples exposed to radiation from laser ablation of transition-metals. New infrared bands are observed in addition to better determination of the vibrational characteristics for the previously reported bands, and the $^{13}C$ substituted isotopomers ($^{13}CH_2{}^{13}CNH$ and $^{13}CH_2N^{13}CH$) are also generated. Density functional frequency calculations and the D and $^{13}C$ isotopic shifts substantiate the vibrational assignments. $CH_2CNH$ is probably produced through single-step conversion of $CH_3CN$, whereas $CH_2NCH$ through two-step conversion *via* 2*H*-azirine. Inter-conversions between these two products evidently do not occur during photolysis and annealing.

**Key Words :** Acetonitrile, Ketenimine, *N*-Methylide, Matrix-infrared, DFT

## Introduction

While Acetonitrile has been a model compound in the development of vibrational spectroscopy,[1] its photo-isomers and fragments have also been the subjects of many spectroscopic and molecular dynamics studies.[1-5] Especially inter-conversions between the cyano and isocyano isomers, formation of the cyclic derivatives, electron-trapping, and C-H bond dissociation have drawn much attention, and their products have been investigated. However, only the strong vibrational bands are observed for many transient species in earlier days,[3-7] and therefore, the information for their vibrational characteristics need to be improved. The higher product yield and enhanced instrumental resolution allow observation of the weaker bands and better determination of their frequencies.[8,9]

UV-photolysis of acetonitrile and dissociation of larger *N*-containing compounds have been the major routes for preparation of the isomers and fragments of acetonitrile.[3,6,7] Jacox has identified $CH_2CNH$ by uv irradiation of acetonitrile and listed three more groups of unidentified product absorptions.[6] Maier *et al.* have succeeded in providing $CH_2NCH$ and several other acetonitrile isomers by photodissociation of vinyl azide ($CH_2CHN_3$).[7] It has also been shown that the radiation from transition-metal plume by laser-ablation is an effective UV source, allowing valuable opportunities to prepare the photo-chemical products during co-deposition with the reagent.[8,9] Recently the cyano and isocyano methyl radicals ($CH_2CN$ and $CH_2NC$) are identified in the acetonitrile spectra along with the weaker absorptions as well as the previously examined strong wagging bands.[8] The DFT results show that the two methyl radicals are easily inter-convertible *via* the cyclic isomer, *cyc*-$CH_2CN$.

In this study, we report matrix IR spectra of $CH_2CNH$ and $CH_2NCH$, which are among the primary isomerization products of acetonitrile. The newly observed absorptions and better determined frequencies are presented, and the $^{13}C$ substituted isotopomers ($^{13}CH_2{}^{13}CNH$ and $^{13}CH_2N^{13}CH$) are also provided. The smallest ketenimine and hydrogen cyanide *N*-methylide are apparently produced *via* two different reaction paths and not inter-convertible.

## Experimental and Computational Methods

Reaction of laser-ablated transition-metal and reagent in excess argon has been an effective route to provide new metal-containing transient species.[10] In these experiments, transition-metal atoms and intense radiation from the laser-ablation plume impinge on the depositing matrix sample, causing photo-isomerization and fragmentation of the reagent.[11] Reagent gas mixtures are typically 0.125-0.500% in argon. The Nd:YAG laser fundamental (1064 nm, 10 Hz repetition rate, 10 ns pulse width) was focused onto the rotating metal target using 5-10 mJ/pulse. After deposition, infrared spectra were recorded at 0.5 $cm^{-1}$ resolution using a Nicolet 550 spectrometer with a Hg-Cd-Te range B detector. Then samples were irradiated for 20 min periods by a mercury arc street lamp (175 W) with the globe removed using a combination of optical filters or annealed to allow further reagent diffusion.

The $H_2CCNH$ and $H_2CNCH$ spectra shown in this report were recorded from samples prepared by co-deposition of laser-ablated Zr (Johnson-Matthey) with acetonitrile isotopomers ($CH_3CN$, $CD_3CN$, and $^{13}CH_3{}^{13}CN$) in excess argon at 10 K using a closed-cycle refrigerator (Air Products, Displex). However, other transition-metals (Groups 3 and 5-8 and actinides) also yield the same $H_2CCNH$ and $H_2CNCH$ absorptions while the relative intensities between $H_2CCNH$ and $H_2CNCH$ vary due to different laser ablation plume radiation from specific metal surfaces.[12] Therefore, these metal independent absorptions do not involve a metal con-

taining species.

Complementary density functional theory (DFT) calculations were also carried out using the Gaussian 09 package,[13] the B3LYP density functional,[14] and 6-311++G(3df,3pd) basis sets for C, H, and N to provide a consistent set of vibrational frequencies and energies for the reaction products and their analogues. Additional BPW91[15] calculations were done to confirm the B3LYP results. Geometries were fully relaxed during optimization, and the optimized geometry was confirmed by vibrational analysis. Every minimum identified on the potential energy surface (PES) was found to have all positive harmonic vibrational frequencies, and each transition state structure to have only one imaginary frequency, corresponding to the reaction coordinate. Intrinsic reaction coordinate (IRC) calculations[16] have been performed to link transition structures with the reactants and products. The vibrational frequencies were calculated analytically, and the zero-point energy is included in the calculation of binding energy of a metal complex.

## Results and Discussion

**Observation of $CH_2CNH$ and $CH_2NCH$.** Figures 1-3 show the matrix IR spectra in $CH_2CNH$ and $CH_2NCH$ absorption regions from co-deposition of Zr with $CH_3CN$, $CD_3CN$, and $^{13}CH_3{}^{13}CN$ and their variation in subsequent photolysis and annealing.[12] Absorptions form other isomers and fragments, particularly $CH_3NC$, $CH_2CN$, and $CH_2NC$, are also observed along with Zr containing products.[2-5] "**CNH**" and "**NCH**" stand for the $CH_2CNH$ and $CH_2NCH$ absorptions in Figures 1-3. The **CNH** absorptions are much stronger than the **NCH** absorptions. They gradually decrease throughout the process of photolysis and annealing, but retain most of their absorption intensities even after annealing at 28 K. On the other hand, the **NCH** absorptions remain almost unchanged on visible ($\lambda > 420$ nm) irradiation, but decrease to about a third the original intensity on uv ($240 < \lambda < 380$ nm) irradiation and gradually decrease in annealing. The observed $H_2CCNH$ and $H_2CNCH$ frequencies are compared with the B3LYP and BPW91 computed values in Tables 1 and 2, and the previously reported values are also listed.[6,7]

The strongest **CNH** CCN *anti*-symmetric stretching absorption and its D counterpart are observed at 2037.2 and 1995.3 $cm^{-1}$ (the previous values of 2040 and 1998 $cm^{-1}$),[6] and the new $^{13}C$ counterpart at 1981.5 $cm^{-1}$. The $^{13}C$ shift larger than the D shift is consistent with the CCN stretching mode, which is in essence vibration of the center C between C and N. The second strong **CNH** A' NCH bending absorp-

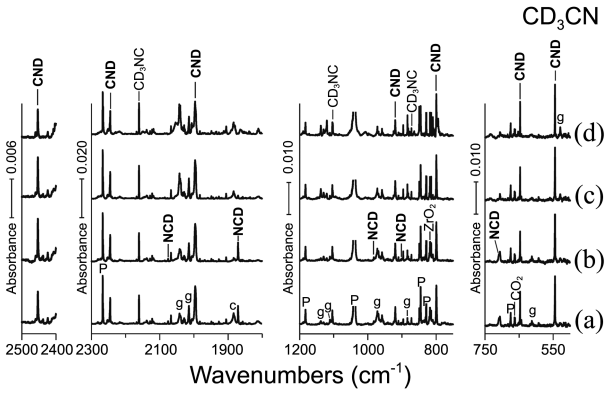


**Figure 2.** IR spectra in the $CD_2CND$ and $CD_2NCD$ absorptions regions for laser-ablated Zr atoms co-deposited with $CD_3CN$ in excess argon at 10 K and their variation. (a) Zr + 0.50% $CD_3CN$ in Ar co-deposited for 1 h. (b) As (a) after photolysis ($\lambda > 420$ nm). (c) As (b) after photolysis ($240 < \lambda < 380$ nm). (d) As (c) after annealing to 28 K. **CND** and **NCD** stand for the $CD_2CND$ and $CD_2NCD$ absorptions, and P, c, and g designate the precursor, common, and Zr + $CD_3CN$ product absorptions. $CH_3NC$, $ZrO_2$, and $CO_2$ absorptions are also indicated.

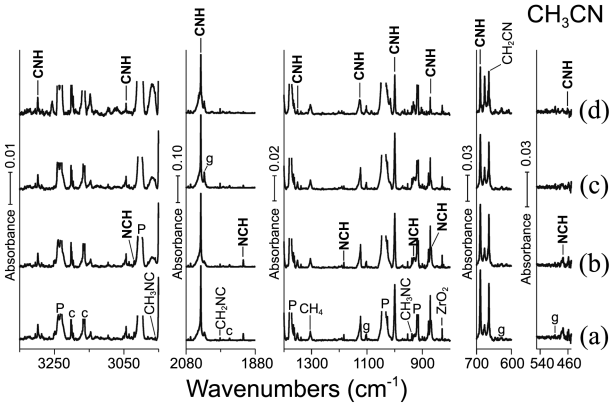


**Figure 1.** IR spectra in the $CH_2CNH$ and $CH_2NCH$ absorption regions for laser-ablated Zr atoms co-deposited with $CH_3CN$ in excess argon at 10 K and their variation. (a) Zr + 0.25% $CH_3CN$ in Ar co-deposited for 1 h. (b) As (a) after photolysis ($\lambda > 420$ nm). (c) As (b) after photolysis ($240 < \lambda < 380$ nm). (d) As (c) after annealing to 28 K. **CNH** and **NCH** stand for the $CH_2CNH$ and $CH_2NCH$ absorptions, and P, c, and g designate the precursor, common, and Zr + $CH_3CN$ product absorptions. $CH_2NC$, $CH_4$, $CH_3NC$, and $ZrO_2$ absorptions are also indicated.

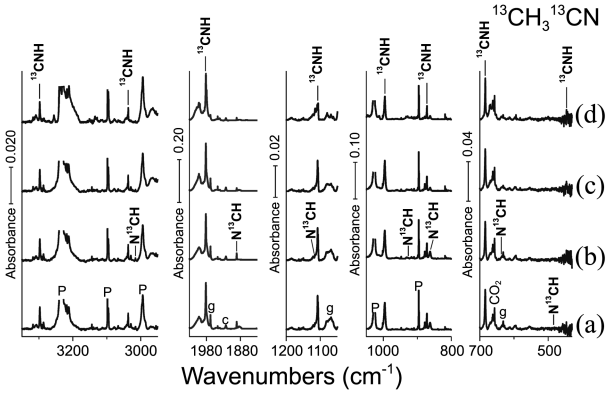


**Figure 3.** IR spectra in the $^{13}CH_2{}^{13}CNH$ and $^{13}CN^{13}CH_2$ absorption regions for laser-ablated Zr atoms co-deposited with $^{13}CH_3{}^{13}CN$ in excess argon at 10 K and their variation. (a) Zr + 0.50% $^{3}CH_3{}^{13}CN$ in Ar co-deposited for 1 h. (b) As (a) after photolysis ($\lambda > 420$ nm). (c) As (b) after photolysis ($240 < \lambda < 380$ nm). (d) As (c) after annealing to 28 K. $^{13}$**CNH** and **N$^{13}$CH** stand for the $^{13}CH_2{}^{13}CNH$ and $^{13}CH_2N^{13}CH$ absorptions, and P, c, and g designate the precursor, common, and Zr + $^{13}CH_3{}^{13}CN$ product absorptions. $CO_2$ absorption is also indicated.

**Table 1.** Calculated Fundamental Frequencies of $CH_2CNH$ Isotopomers in the Ground $^1A'$ State[a]

| Approximate Description | $CH_2CNH$ | | | | | $CD_2CND$ | | | | | $^{13}CH_2{}^{13}CNH$ | | | | |
|---|---|---|---|---|---|---|---|---|---|---|---|---|---|---|---|
| | Obs[b] | B3LYP[c] | Int[c] | BPW91[d] | Int[d] | Obs[b] | B3LYP[c] | Int[c] | BPW91[d] | Int[d] | Obs[b] | B3LYP[c] | Int[c] | BPW91[d] | Int[d] |
| A' N-H str. | 3297.8 | 3477.6 | 22 | 3393.8 | 12 | 2452.9 | 2553.7 | 42 | 2491.8 | 27 | 3297.5 | 3477.6 | 22 | 3393.8 | 11 |
| A" $CH_2$ as. str. | | 3250.6 | 1 | 3193.1 | 1 | | 2420.4 | 0 | 2377.0 | 0 | | 3237.3 | 1 | 3180.0 | 1 |
| A' $CH_2$ s. str. | 3043.5 | 3164.2 | 9 | 3107.1 | 8 | 2245.3 | 2318.1 | 71 | 2275.9 | 61 | 3036.8 | 3158.1 | 8 | 3101.1 | 7 |
| A' CCN as. str. | 2037.2, 2040[e] | 2115.5 | 436 | 2070.8 | 370 | 1995.3, 1998[e] | 2072.9 | 385 | 2029.3 | 332 | 1981.5 | 2050.2 | 410 | 2006.8 | 347 |
| A' $CH_2$ scis. | 1350.7 | 1439.6 | 5 | 1388.0 | 6 | covered | 1251.8 | 1 | 1215.5 | 1 | 1337.8 | 1427.0 | 6 | 1375.3 | 8 |
| A' CCN s. str. | 1123.4, 1124[e] | 1166.5 | 18 | 1136.5 | 16 | 919.9, 921[e] | 947.6 | 23 | 916.8 | 23 | 1108.5 | 1150.5 | 18 | 1121.3 | 15 |
| A' NCH bend | 999.6, 1000[e] | 1025.3 | 210 | 1000.0 | 196 | 799.4, 800[e] | 815.2 | 86 | 792.4 | 79 | 995.6 | 1020.7 | 210 | 995.7 | 196 |
| A" $CH_2$ rock | | 1001.0 | 0 | 962.0 | 0 | | 850.4 | 0 | 818.4 | 0 | | 984.3 | 0 | 945.8 | 0 |
| A" N-H tort | 871.6, 872[e] | 896.6 | 53 | 872.4 | 49 | 647.2, 648[e] | 661.2 | 30 | 643.3 | 28 | 871.5 | 896.4 | 53 | 872.2 | 49 |
| A' $CH_2$ wag | 689.2, 690[e] | 717.7 | 87 | 665.7 | 86 | 544[g] | 569.7 | 45 | 527.0 | 42 | 684.0 | 711.3 | 87 | 660.2 | 85 |
| A' CCN ip bend | 458.1 | 484.1 | 22 | 468.1 | 20 | | 429.4 | 30 | 417.7 | 30 | 446.3[f] | 470.7 | 19 | 454.9 | 18 |
| A" CCN oop bend | | 421.9 | 0 | 407.0 | 1 | | 361.1 | 0 | 347.6 | 1 | | 413.6 | 0 | 399.1 | 1 |

[a]Frequencies and intensities are in $cm^{-1}$ and km/mol. Frequencies and intensities are computed with 6-311++G(3df, 3pd) for harmonic calculations. [b]Observed in an argon matrix. [c]Computed with B3LYP. [d]Computed with BPW91. [e]Ref 6. [f]Tantative assignment. [g]Overlapped with a $CH_2CN$ band. $CH_2CNH$ has a $C_s$ structure.

tion and its D counterpart are observed at 999.6 and 799.4 $cm^{-1}$ (close to the reported values of 1000 and 800 $cm^{-1}$), and $^{13}C$ substitution shifts it to 995.6 $cm^{-1}$. The third strong A' $CH_2$ wagging band at 689.2 $cm^{-1}$ (the previous frequency of 690 $cm^{-1}$) shifts to 544 and 684 $cm^{-1}$ on deuteration and $^{13}C$ substitution. The N-H torsion and CCN symmetric stretching frequencies and their D counterparts are also close to the previously reported values and the $^{13}C$ counterparts observed. The five previously reported frequencies[6] are all slightly higher (0.4-2.8 $cm^{-1}$) than the measured frequencies in this study. The newly observed frequencies of the $^{13}CH_2{}^{13}CNH$ show good correlation with the DFT values as shown in Table 1.

Four weaker **CNH** absorptions are newly observed as well. The one at 3297.8 $cm^{-1}$ shifts to 2452.9 and 3297.5 $cm^{-1}$ on deuteration and $^{13}C$ substitution (H/D ratios of 1.344). The high frequency, large D shift, and negligible $^{13}C$ shift lead to an assignment to the N-H stretching mode of $CH_2CNH$. The **CNH** absorption at 3043.5 $cm^{-1}$ is designated to the $CH_2$ symmetric stretching mode with its D and $^{13}C$ counterparts at 2245.3 and 3036.8 $cm^{-1}$ (H/D ratio of 1.355). The one at 1350.7 $cm^{-1}$ is assigned to the $CH_2$ scissoring mode with its $^{13}C$ counterpart at 1337.8 $cm^{-1}$, and the absorption at 458.1 $cm^{-1}$ is assigned to the CCN in-plane

**Table 2.** Calculated Fundamental Frequencies of $CH_2NCH$ Isotopomers in the Ground $^1A'$ State[a]

| Approximate Description | $CH_2NCH$ | | | | | $CD_2NCD$ | | | | | $^{13}CH_2N^{13}CH$ | | | | |
|---|---|---|---|---|---|---|---|---|---|---|---|---|---|---|---|
| | Obs[b] | B3LYP[c] | Int[c] | BPW91[d] | Int[d] | Obs[b] | B3LYP[c] | Int[c] | BPW91[d] | Int[d] | Obs[b] | B3LYP[c] | Int[c] | BPW91[d] | Int[d] |
| A" $CH_2$ as. str. | | 3246.0 | 1 | 3188.3 | 1 | | 2423.7 | 2 | 2380.0 | 1 | | 3232.0 | 1 | 3174.6 | 1 |
| A' $CH_2$ s. str. | | 3141.5 | 2 | 3084.9 | 2 | 2075.3 | 2279.2 | 12 | 2238.0 | 11 | | 3136.5 | 1 | 3079.9 | 1 |
| A' C-H str. | 3019.5 | 3099.1 | 3 | 3057.3 | 3 | covered | 2311.1 | 13 | 2285.2 | 16 | 3015.4 | 3089.0 | 4 | 3047.2 | 4 |
| A' CNC as. str. | 1914.7, 1914.5[e] | 1996.7 | 266 | 1988.0 | 250 | 1870.5, 1869.4 sh, 1870.2[e] | 1944.3 | 296 | 1932.6 | 270 | 1890.8 | 1972.5 | 251 | 1963.5 | 237 |
| A' $CH_2$ scis. | | 1502.9 | 4 | 1447.3 | 5 | | 1301.2 | 1 | 1261.0 | 0 | | 1489.2 | 5 | 1433.8 | 6 |
| A' CNC s. str. | 1183.7, 1183.6[e] | 1232.9 | 8 | 1199.7 | 5 | 982.8, 982.6[e] | 1002.6 | 11 | 969.8 | 10 | 1172.0 | 1195.9 | 7 | 1164.0 | 4 |
| A" $CH_2$ rock | 1127.4, 1127.3[e] | 1147.9 | 7 | 1103.3 | 5 | 900.5, 900.1[e] | 918.0 | 6 | 883.8 | 4 | 1116.3 | 1139.4 | 7 | 1095.2 | 5 |
| A" $CH_2$ tort | 927.6 | 965.2 | 11 | 921.9 | 12 | | 719.0 | 7 | 686.3 | 8 | 925.1 | 961.5 | 11 | 918.4 | 11 |
| A' NCH bend | 868.5, 866.3[e] | 910.2 | 375 | 872.3 | 317 | 709.6, 708.0sh, 708.3[e] | 737.1 | 175 | 704.4 | 149 | 862.1 | 903.2 | 373 | 865.7 | 316 |
| A' $CH_2$ wag | 639.6[f] | 735.6 | 79 | 654.0 | 98 | 520.1[f] | 589.0 | 35 | 527.1 | 34 | 635.8[f] | 728.8 | 79 | 648.1 | 99 |
| A' CNC in bend | 473.5, 473.5[e] | 489.9 | 32 | 468.3 | 33 | 414.6[e] | 427.2 | 49 | 406.3 | 56 | 466.7[f] | 486.2 | 31 | 464.6 | 30 |
| A" CNC oop bend | | 350.5 | 4 | 336.5 | 2 | | 315.4 | 2 | 302.6 | 1 | | 347.6 | 4 | 334.0 | 2 |

[a]Frequencies and intensities are in $cm^{-1}$ and km/mol. Frequencies and intensities are computed with 6-311++G(3df, 3pd) for harmonic calculations. [b]Observed in an argon matrix. [c]Computed with B3LYP. [d]Computed with BPW91. [e]Ref 7. [f]Tentative assignment. sh indicates shoudler. $CH_2NCH$ has a $C_s$ structure.

bending mode. The 9 vibrational bands of $CH_2CNH$ with sizable absorption intensities are all observed in this study as shown in Table 1.

Though much weaker, the **NCH** absorptions are still readily distinguishable with their large decrease in absorption intensity on uv ($240 < \lambda < 380$ nm) irradiation. The five previously reported $CH_2NCH$ vibrational bands are again the strongest ones in our spectra. These absorptions are observed close (slightly higher) to the previous values. The strongest NCH bending absorption and its D counterpart are observed at 868.5 and 709.6 $cm^{-1}$ (the previous values are 866.3 and 708.3 $cm^{-1}$), and the $^{13}C$ counterpart at 862.1 $cm^{-1}$. The second strongest CNC *anti*-symmetric stretching band and its D counterpart at 1914.7 and 1870.5 $cm^{-1}$ are also compared with the previous values of 1914.5 and 1870.2 $cm^{-1}$ and carry the $^{13}C$ counterpart at 1890.8 $cm^{-1}$. The weaker CNC symmetric stretching, $CH_2$ rocking, and NCH bending absorptions are also observed near the previously reported values along with the new $^{13}C$ counterparts.

Jacox has performed microwave-discharge of Ar/$CH_3CN$ (Ar radiation of 121.6 nm) and subsequent mercury-arc photolysis ($\lambda > 250$ nm) and classified the product absorptions into Groups A-D on the basis of their behavior on photolysis.[6] The author has assigned Group B to $CH_2CNH$ while leaving the other three groups unidentified. It is worthy to mention at this point that among the three groups, Group A belongs to $CH_2NCH$, the CNC *anti*-symmetric stretching, $CH_2$ rocking, and NCH bending absorptions, and Groups C and D to $CH_2CN$ and $CH_2NC$.[8] This is consistent with our results that both the smallest ketenimine and hydrogen cyanide *N*-methylide are generated along with $CH_2CN$ and $CH_2NC$ by photolysis of argon/acetonitrile matrix sample.

Four weaker **NCH** absorptions are also observed. The ones at 3019.5 and 927.6 $cm^{-1}$ are accompanied with their $^{13}C$ counterparts at 3015.4 and 925.1 $cm^{-1}$ and are designated to the C-H stretching and $CH_2$ torsion mode without observation of the D counterparts. The B3LYP and BPW91 $CH_2$ wagging frequencies (735.6 and 654.0 $cm^{-1}$) show a large difference. The weak absorption at 639.6 $cm^{-1}$ is tentatively assigned to the $CH_2$ wagging mode with the D and $^{13}C$ counterparts at 520.1 and 635.8 $cm^{-1}$. Another **NCH** absorption at 2075.3 $cm^{-1}$ in the $CD_3CN$ spectra are assigned to the $CH_2$ symmetric stretching mode without observation of its isotopic counterparts. These 9 product absorptions and consistency with the previous results substantiate production of $CH_2NCH$.

**Reactions in the Matrix.** $CH_2CNH$ and $CH_2NCH$, 92 and 212 kJ/mol higher than $CH_3CN$, are the major photo-isomerization products of acetonitrile along with $CH_3NC$ observed in the matrix IR spectra (Figures 1-3).[2,6,12] The B3LYP structures of $CH_2CNH$ and $CH_2NCH$ are shown in Figure 4. Both products own the 1A' ground electronic states and similar $C_s$ structures. $CH_2CNH$ is most probably produced by single step conversion of acetonitrile as shown in Figure 5. One of the methyl H migrates to N while the remaining molecular structure ($CH_2CN$) is largely preserved. TS1 (The transition state for $CH_3CN \rightarrow CH_2CNH$) is 369 kJ/mol higher than $CH_3CN$ (Figure 5). Multi-step conversions *via* the plausible isomers of acetonitrile such as azirine and methyl isocyanide are also examined, but they are energetically unfavorable and the transition states also do not lead to the product according to our IRC analyses.

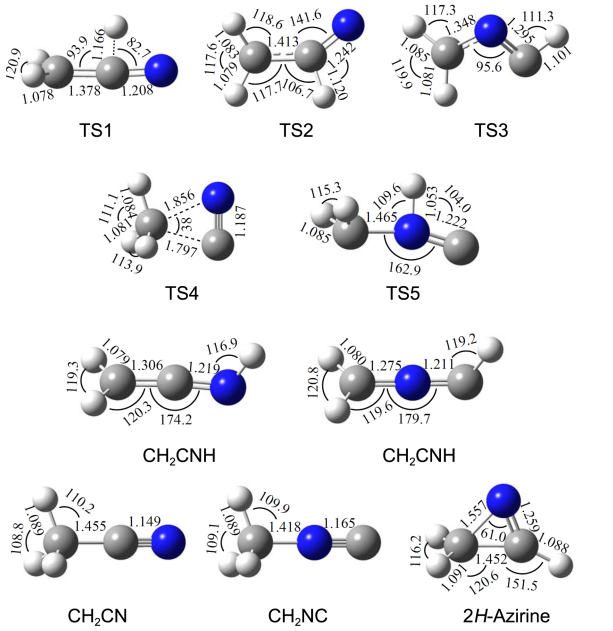


**Figure 4.** The B3LYP structures of $CH_2CNH$, $CH_2NCH$, $CH_3CN$, $CH_3NC$, 2*H*-azirine, and TS1-5. $CH_2CNH$, $CH_2NCH$, and 2*H*-azirine own $C_s$ structures, and $CH_3CN$ and $CH_3NC$ $C_{3v}$ structures. TS1, TS4, and TS5 possess $C_s$ structures while TS2 and TS3 $C_1$ structures. The bond lengths and angles are in Å and degrees.

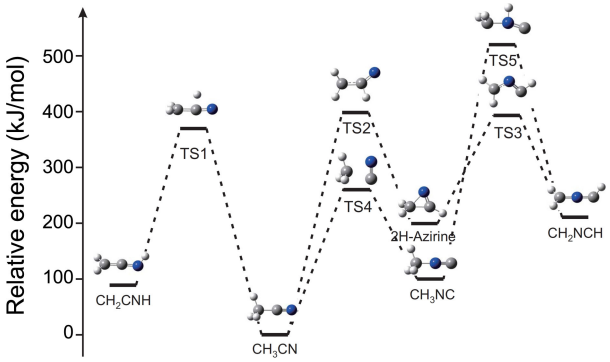


**Figure 5.** The relative energies of $CH_2CNH$, $CH_2NCH$, $CH_3CN$, $CH_3NC$, 2*H*-azirine, and the transition states between them in the singlet potential energy surface. $CH_2CNH$, $CH_2NCH$, $CH_3NC$, and 2*H*-azirine are 92, 212, 98, and 199 kJ/mol higher than $CH_3CN$, respectively, and TS1-5 are 369, 397, 394, 261, and 520 kJ/mol higher than $CH_3CN$.

On the other hand, conversion of acetonitrile to $CH_2NCH$ probably occurs in two steps, $CH_3CN \rightarrow$ 2*H*-azirine (*cyc*-$CH_2NCH$) $\rightarrow CH_2NCH$. The transition state between $CH_3CN$ and 2*H*-azirine (TS2) is 397 kJ/mol higher than acetonitrile and has a near planar structure in contrast to the structure of TS1. 2*H*-azirine is known to readily convert to other products on photolysis or to undergo reactions with a variety of reagents to form more complex products.[7] Ring-opening

(breaking the C-C bond) results in generation of $CH_2NCH$ through TS3. Another possible reaction path is *via* methyl isocyanide, which is one of the primary products, $CH_3CN \rightarrow CH_3NC \rightarrow CH_2NCH$. However, its energetically high transition state (TS5), which is 520 and 422 kJ/mol higher than $CH_3CN$ and $CH_3NC$, respectively, makes the reaction path less favorable.

Inter-conversions between $CH_2CNH$ and $CH_2NCH$ apparently do not occur unlike the previously studied $CH_2CN$-$CH_2NC$ case.[8] The dramatic decrease of **NCH** absorptions on uv irradiation is not accompanied with increase of the **CNH** absorptions. In fact, the two sets of product absorptions continuously decrease in the process of photolysis and annealing while the extents of variation differ each other. Inter-conversions would result in an increase of a product and a decrease of the other. Inter-conversions between these two species would occur probably *via* cyclic configurations ($CH_2CNH \leftrightarrow$ *cyc*-$CH_2CNH \leftrightarrow$ *cyc*-$CH_2NCH \leftrightarrow CH_2NCH$). *Cyc*-$CH_2NHC$ is 119 kJ/mol higher in energy than *cyc*-$CH_2NCH$ (2*H*-azirine), and the transition states between the species along the reaction path are 388, 369, and 303 kJ/mol higher in energy than $CH_2CNH$, suggesting that the three-step isomerization is not efficient.

2*H*-azirine is illusive in matrix-IR spectra, due to its low stability and relatively low absorption intensities.[6,7] Maier *et al.* have reported provision of this small *N*-containing cyclic compound by photo-dissociation of vinyl azide ($CH_2CHN_3$) without observation of its isotopomers.[7] Weak product absorptions are observed at 972.4, 1228.4, and 772.4 $cm^{-1}$ in this study near the reported $CH_2$ rocking, C-C stretching, and C-H out-of-plane bending frequencies, the strongest bands of the complex. No more attempts have been made to identify this product due to the low absorption intensities.

## Conclusions

The smallest ketenimine and hydrogen cyanide *N*-methylide ($CH_2CNH$ and $CH_2NCH$) are observed in the infrared spectra of argon/acetonitrile matrix samples prepared under exposure to laser-ablation irradiation. The frequencies of the strongest five absorptions are near the previously reported values for each species and four more absorptions are newly observed. The frequencies of the $^{13}C$ substituted isotopomers are also reported, and the observed frequencies correlate well with the DFT computed values. DFT results also reveal that $CH_2CNH$ is most probably produced in a single-step conversion from $CH_3CN$, whereas $CH_2NCH$ in a two-step reaction *via* 2*H*-azirine. The $CH_2NCH$ absorptions dramatically decrease on uv irradiation while the $CH_2CNH$ also decrease gradually in the process of photolysis and annealing, indicating that these two acetonitrile isomers are not readily inter-convertible. Computation results for the plausible inter-conversion reaction path also support the observed results.

**Acknowledgments.** This work is partially supported by University of Incheon Research Grant in 2011.

## References and Notes

1. (a) Sandholm, S. T.; Bjarnov, E.; Schwendeman, R. H. *J. Mol. Spectrosc*. **1982**, *95*, 276-287. (b) Kukolich, S. G. *J. Chem. Phys*. **1982**, *76*, 997-1006. (c) Sassi, P.; Paliani, G.; Cataliotti, R. S. *J. Chem. Phys*. **1998**, *108*, 10197-10205.
2. (b) Deng, R.; Trenary, M. *J. Phys. Chem. C* **2007**, *111*, 17088-17093. (MeCN isomers). (b) Yang, X.; Maeda, S.; Ohno, K. *J. Phys. Chem. A* **2005**, *109*, 7319-7358. (c) Fan, L.; Ziegler, T. *J. Chem. Phys.* **1990**, *92*, 3645-3652. (PES of $CH_3CN$). (d) Hattori, R.; Suzuki, E.; Shimizu, K. *J. Mol. Struct*. **2005**, *738*, 165-170. ($CH_3NC$).
3. (a) Moran, S.; Ellis, H. B., Jr.; DeFrees, D. J.; McLean, A. D.; Ellison, G. B. *J. Am. Chem. Soc.* **1987**, *109*, 5996-6003. (b) Svejda, P.; Volman, D. H. *J. Phys. Chem*. **1970**, *74*, 1872-1875. (c) Egland, R. J.; Symons, M. R. C. *J. Chem. Soc. A* **1970**, *5*, 1326-1329. ($H_2CCN$).
4. (a) Moran, S.; Ellis, H. B., Jr.; DeFrees, D. J.; McLean, A. D.; Paulson, S. E.; Ellison, G. B. *J. Am. Chem. Soc*. **1987**, *109*, 6004-6010. (b) Hirao, T.; Ozeki, H.; Saito, S.; Yamamoto, S. *J. Chem. Phys*. **2007**, *127*, 134312-1-7. ($H_2CNC$).
5. (a) Maier, G.; Reisenauser, H. P.; Rademacher, K. *Chem. Eur. J.* **1998**, *4*, 1957-1963. (b) Dendramis, A.; Leroi, G. E. *J. Chem. Phys*. **1977**, *66*, 4334-4341. (c) Nimlos, M. R.; Davico, G.; Geise, C. M.; Wenthold, P. G.; Blanksby, W. C.; Lineberger, S. J.; Hadad, C. M.; Petersson, G. A.; Ellison, G. B. *J. Chem. Phys*. **2002**, *117*, 4323-4340. (d) Jacox, M. E. *J. Phys. Chem. Ref. Data* **2003**, *32*, 1-441. (HCCN, HCNC, & cyc-HCNC).
6. (a) Jacox, M. E. *Chem. Phys*. **1979**, *43*, 157-172. (b) Jacox, M. E.; Milligan, D. E. *J. Am. Chem. Soc*. **1963**, *85*, 278-282.
7. Maier, G.; Schmidt, C.; Reisenauer, H. P.; Endlein, E.; Becker, D; Eckwert, J.; Hess, B. A.; Schaad, L. J. *Chem. Ber*. **1993**, *126*, 2337-2352.
8. Cho, H.-G.; Andrews, L. *J. Phys. Chem*. **2011**, *115*, 8638-8642.
9. Andrews, L.; Kushto, G. P.; Zhou, M.; Willson, S. P.; Souter, P. F. *J. Chem. Phys*. **1999**, *110*, 4457-4466.
10. (a) Andrews, L.; Cho, H.-G. *Organometallics* **2006**, *25*, 4040-4053. (Review article). (b) Cho, H.-G.; Andrews, L. *J. Am. Chem. Soc*. **2008**, *130*, 15836-15841. (c) Zhou, M.; Chen, M.; Zhang, L.; Lu, H. *J. Phys. Chem. A* **2002**, *106*, 9017-9023. (d) Cho, H.-G.; Andrews, L. *Dalton Trans*. **2011**, *40*, 11115-11124.
11. (a) Andrews, L.; Citra, A. *Chem. Rev.* **2002**, *102*, 885-911, and references therein. (b) Andrews, L. *Chem. Soc. Rev.* **2004**, *33*, 123-132, and references therein.
12. (a) Cho, H.-G.; Andrews, L. *J. Phys. Chem. A* **2010**, *114*, 891-897. (b) Cho, H.-G.; Andrews, L. *J. Phys. Chem. A* **2010**, *114*, 5997-6006. (c) Cho, H.-G.; Andrews, L. *J. Organomet. Chem*. **2012**, *703*, 25-33. (d) Cho, H.-G.; Andrews, L. *Organometallics* **2011**, *31*, 535-544.
13. Frisch, M. J.; Trucks, G. W.; Schlegel, H. B.; Scuseria, G. E.; Robb, M. A.; Cheeseman, J. R.; Scalmani, G.; Barone, V.; Mennucci, B.; Petersson, G. A.; *et al. Gaussian 09*, Revision A.02, Gaussian, Inc.: Wallingford, CT, 2009.
14. (a) Becke, A. D. *J. Chem. Phys.* **1993**, *98*, 5648-5652. (b) Lee, C.; Yang, Y.; Parr, R. G. *Phys. Rev. B* **1988**, *37*, 785-789.
15. Burke, K.; Perdew, J. P.; Wang, Y. In *Electronic Density Functional Theory: Recent Progress and New Directions*; Dobson, J. F., Vignale, G., Das, M. P., Eds.; Plenum: 1998.
16. Fukui, K. *Acc. Chem. Res*. **1981**, *14*, 363-368.